Centrality evolution of the charged-particle pseudorapidity density over a broad pseudorapidity range in Pb-Pb collisions at √sNN = 2.76 TeV

(ALICE Collaboration) Adam, J.; ...; Antičić, Tome; ...; Erhardt, Filip; ...; Gotovac, Sven; ...; Mudnić, Eugen; ...; ...

Centrality evolution of the charged-particle pseudorapidity density over a broad pseudorapidity range in Pb–Pb collisions at $\sqrt{s_{\mathrm{NN}}} = 2.76$ TeV

ALICE Collaboration *

ABSTRACT

The centrality dependence of the charged-particle pseudorapidity density measured with ALICE in Pb–Pb collisions at $\sqrt{s_{\mathrm{NN}}} = 2.76$ TeV over a broad pseudorapidity range is presented. This Letter extends the previous results reported by ALICE to more peripheral collisions. No strong change of the overall shape of charged-particle pseudorapidity density distributions with centrality is observed, and when normalised to the number of participating nucleons in the collisions, the evolution over pseudorapidity with centrality is likewise small. The broad pseudorapidity range ($-3.5 < \eta < 5$) allows precise estimates of the total number of produced charged particles which we find to range from $162 \pm 22(\mathrm{syst.})$ to $17170 \pm 770(\mathrm{syst.})$ in 80–90% and 0–5% central collisions, respectively. The total charged-particle multiplicity is seen to approximately scale with the number of participating nucleons in the collision. This suggests that hard contributions to the charged-particle multiplicity are limited. The results are compared to models which describe $\mathrm{d}N_{\mathrm{ch}}/\mathrm{d}\eta$ at mid-rapidity in the most central Pb–Pb collisions and it is found that these models do not capture all features of the distributions.

1. Introduction

The measurement of the charged-particle pseudorapidity (η) density distribution in heavy-ion collisions provides insight into the dominant particle production mechanisms, such as parton fragmentation [1] and the observed phenomenon of limiting fragmentation [2]. The unique capability of ALICE to perform such measurements from large to small overlaps of the colliding nuclei over a broad pseudorapidity range allows for significant additional information to be extracted e.g., the total number of charged particles and the evolution of the distributions with centrality.

The charged-particle pseudorapidity density ($\mathrm{d}N_{\mathrm{ch}}/\mathrm{d}\eta$) *per se* does not provide immediate understanding of the particle production mechanism, but as a benchmark tool for comparing models it is indispensable. Various models [3–5] make different assumptions on how particles are produced in heavy-ion collisions resulting in very different charged-particle pseudorapidity density distributions — both in terms of scale and shape. Models may, for example, incorporate different schemes for the hadronisation of the produced quarks and gluons which leads to very different pseudorapidity distributions of the charged particles.

The ALICE Collaboration has previously reported results on the charged-particle pseudorapidity density in the 0–30% most central Pb–Pb collisions at $\sqrt{s_{\mathrm{NN}}} = 2.76$ TeV over a wide pseudorapidity range [6], and in the 80% most central collisions at mid-rapidity ($\eta \approx 0$) only [7]. The ATLAS Collaboration has reported on the charged-particle pseudorapidity density in the 80% most central events in a limited pseudorapidity range of $|\eta| < 2$ [8]. Similarly, the CMS Collaboration has reported on the same measurements in the 90% most central events at $\eta \approx 0$, and for selected centralities up to $|\eta| < 2$ [9].

In this Letter we present the primary charged-particle pseudorapidity density dependence on the event centrality from mid-central (30–40%) to peripheral (80–90%) collisions over a broad pseudorapidity range to complement results previously reported by ALICE in the 0–30% centrality range. Unlike previous [6], in the forward regions where the signal is dominated by secondary particles produced in the surrounding material, we use a data-driven correction to extract the primary charged-particle density.

Primary charged particles are defined as prompt charged particles produced in the collision, including their decay products, but excluding products of weak decays of muons and light flavour hadrons. Secondary charged particles are all other particles observed in the experiment e.g., particles produced through interactions with material and products of weak decays.

* *E-mail address:* alice-publications@cern.ch.

In the following section, the experimental set-up will be briefly described. Section 3 outlines analysis procedures and describes a data-driven method to isolate the number of primary charged particles from the secondary particle background at large pseudorapidity. Systematic uncertainties are discussed in Sect. 4. In Sect. 5, the resultant charged-particle pseudorapidity density distributions are presented along with their evolution with centrality. Furthermore we extract from the measured $dN_{ch}/d\eta$ distributions the total number of charged particles as a function of the number of participating nucleons. We finally compare the measured charged-particle pseudorapidity density to a number of model predictions before concluding in Sect. 6.

2. Experimental setup

A detailed description of ALICE can be found elsewhere [10,11]. In the following we briefly describe the detectors relevant to this analysis.

The Silicon Pixel Detector (SPD) is the inner-most detector of ALICE. The SPD consists of two cylindrical layers of 9.8×10^6 silicon-pixels possessing binary read-out. It provides a measurement of charged particles over $|\eta| < 2$ using so-called *tracklets* — a combination of hits on each of the two layers (1 and 2) consistent with a track originating from the interaction point. Possible combinations of hits not consistent with primary particles can be removed from the analysis, with only a small (a few %) residual correction for secondary particles derived from simulations. The SPD also provides a measurement, by combining hits on its two layers, of the offset with respect to the interaction point, where the collisions occurred. $\mathbf{IP} = (0, 0, 0)$ is at the centre of the ALICE coordinate system, and IP_z is the offset along the beam axis. Finally, a hardware logical *or* of hits in each of the two layers provides a trigger for ALICE.

The Forward Multiplicity Detector (FMD) is a silicon strip detector with 51 200 individual read-out channels recording the energy deposited by particles traversing the detector. It consists of three sub-detectors FMD1, 2, and 3, placed approximately 320 cm, 79 cm and −69 cm along the beam line, respectively. FMD1 consists of one inner type ring (1i), while both FMD2 and 3 consist of inner (2i, 3i) and outer type rings (2o, 3o). The rings have almost full coverage in azimuth (φ), and high granularity in the radial (η) direction (see Table 1).

The V0 is the most forward of the three detectors used in this analysis. It consists of two sub-detectors: V0-A and V0-C placed at approximately 333 cm and −90 cm along the beam line, respectively. Each of the sub-detectors are made up of scintillator tiles with a high timing resolution. While the V0 provides pulse-height measurements, the energy-loss resolution is not fine enough to do an independent charged particle measurement. In previous measurements, using so-called satellite–main collisions (see Sect. 3), one could match the V0 amplitude to the SPD measurements to obtain a relative measurement of the number of charged particles. However, for collisions at $|IP_z| < 15$ cm no such matching is possible, and the V0 is therefore not used to provide a measurement of the number of charged particles in this analysis. The detector is used, in an inclusive logical *or* with the SPD, for triggering ALICE and to provide a measure of the event centrality [7].

Details on the coverage, resolution, and segmentation of the three used detectors are given in Table 1.

3. Data sample and analysis method

The results presented in this paper are based on Pb–Pb collision data at $\sqrt{s_{NN}} = 2.76$ TeV taken by ALICE in 2010. About 100 000

Table 1

Overview of the resolution (δ), segmentation (Δ), and coverage of the detectors used in the analysis. The 'A' side corresponds to $z > 0$, while the 'C' side corresponds to $z < 0$. The η range is specified for collisions with $IP_z = 0$.

Detector	$\delta r\varphi$	δz	η range
SPD1	12 μm	100 μm	−2.0 to 2.0
2	12 μm	100 μm	−1.4 to 1.4

Detector	$\Delta\varphi$	Δr	η range
FMD1i	18°	254 μm	3.7 to 5.0
2i	18°	254 μm	2.3 to 3.7
2o	9°	508 μm	1.7 to 2.3
3o	9°	508 μm	−2.3 to −1.7
3i	18°	254 μm	−3.4 to −2.0
V0-A	45°	34 to 186 mm	2.8 to 5.1
-C	45°	26 to 127 mm	−3.7 to −1.7

events with a minimum bias trigger requirement [7] were analysed in the centrality range from 0% to 90%. The data was collected over roughly 30 minutes where the experimental conditions did not change.

The standard ALICE event selection [12] and centrality estimator based on the V0-amplitude are used in this analysis [13]. We include here the 80–90% centrality class which was not present in the previous results [7]. As discussed elsewhere [13], the 90–100% centrality class has substantial contributions from QED processes and is therefore not included in this Letter.

Results in the mid-rapidity region ($|\eta| < 2$) are obtained from a tracklet analysis using the two layers of the SPD as mentioned in Sect. 2. The analysis method and data used are identical to what has previously been presented [6,7].

The measurements in the forward region ($|\eta| > 2$) are provided by the FMD. The FMD records the full energy deposition of charged particles that impinge on the detector. Since all charged particles that hit the FMD are boosted in the laboratory frame, the detection efficiency is close to 100% for all momenta. As reported earlier [6], the main challenge in measuring the number of charged primary particles in this region, is the large background of secondary particles produced in the surrounding material. Due to the complexity and the limited knowledge of the material distribution of support structures away from the central barrel, it has not been possible to adequately describe (on the few %-level) the generation of secondary particles in the forward directions within the precision of the current simulation of the ALICE apparatus.

A suitable means to extract the number of primary charged particles was found by utilising collisions between so-called 'satellite' bunches and main bunches offset in intervals of 37.5 cm along the beam-line. Satellite bunches are caused by the so-called debunching effect [14]. A small fraction of the beam can be captured in unwanted RF buckets, due the way beams are injected into the accelerator, and create these satellite bunches spaced by 2.5 ns. Collisions between satellite and main bunches can cause instabilities in the beam, and the LHC has taken steps to reduce the number of these kinds of collisions. ALICE has therefore not recorded collisions between satellite and main bunches before or after the Pb–Pb run of 2010. In satellite–main collisions the background of secondary particles was much smaller and much better understood since significantly less detector material shadows the forward detectors [6].

A study utilising these satellite–main collisions led to the publication of the measurement of the charged-particle pseudorapidity density in the 30% most central events over $|\eta| < 5$ [6]. The study was limited in centrality reach by the need to use the Zero-Degree Calorimeter (ZDC) for the centrality estimation for collisions between satellite and main bunches. The ZDC measures the energy of spectator (non-interacting) nucleons with two components: one
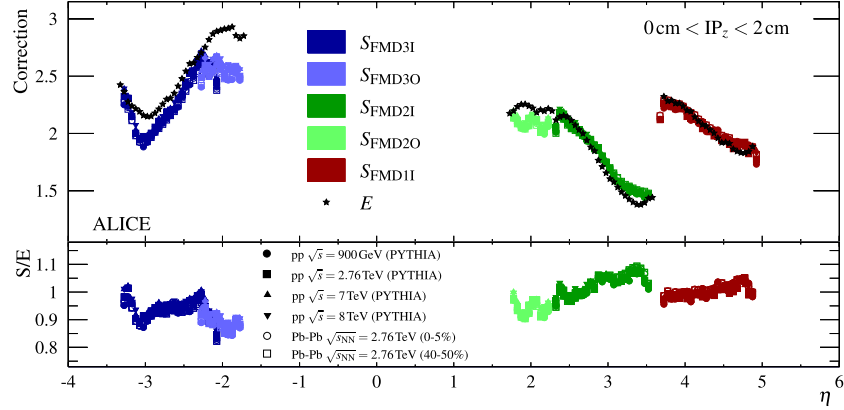
Fig. 1. (Colour online.) Comparison of data-driven to simulation-based corrections for secondary particles impinging on the FMD. Different markers correspond to different collision systems and energies, and the colours indicate the five FMD rings. $S(\eta)$ is shown for 0 cm $<$ IP$_z$ $<$ 2 cm as an example, while $E(\eta)$ is independent of IP$_z$ (see also text). PYTHIA was used for pp collisions, and the Pb–Pb points are from simulation with a parameterisation which include the available ALICE data on particle composition and p_T distributions. Black circles correspond to $E(\eta)$.

measures protons and the other measures neutrons. The ZDC was located at about 114 m from the interaction point on either side of the experiment [10], and was therefore ideally suited for that study. The centrality determination capability of the ZDC is however limited to the 30% most central collisions [13].

For centralities larger than 30% the V0 amplitude is used as the centrality estimator, which is available only for collisions at |IP$_z$| $<$ 15 cm − the so-called nominal interaction point corresponding to main bunches of one beam colliding with main bunches of the other beam.

To extend the centrality reach of the dN_{ch}/dη measurement, a *data-driven* correction for the number of secondaries impinging on the FMD has been implemented. For each centrality class C, we form the ratio

$$E_C(\eta) = \frac{\mathrm{d}N_{ch}/\mathrm{d}\eta|_{C,\mathrm{inclusive,nominal}}}{\mathrm{d}N_{ch}/\mathrm{d}\eta|_{C,\mathrm{primary,satellite}}} \quad . \tag{1}$$

That is, the ratio of the *measured inclusive* charged-particle density from main–main collisions (|IP$_z$| $<$ 10 cm) provided by the FMD to the *primary* charged-particle density from satellite–main collisions [6]. Here, 'inclusive' denotes primary *and* secondary charged particles i.e., no correction was applied to account for secondary particles impinging on the FMD.

Note, that the correction is formed bin-by-bin in pseudorapidity, so that the pseudorapidity is the same for both the numerator and denominator. However, the numerator and denominator differ in the offset along the beam line of origin of the measured particles: For the numerator the origin lies within the nominal interaction region, while for the denominator the origin was offset by multiples of 37.5 cm.

This ratio is obtained separately for all previously published centrality classes: 0–5%, 5–10%, 10–20% and 20–30%. The variation of E_c for different centralities is small ($<$1%, much smaller than the precision of the measurements). The weighted average

$$E(\eta) = \frac{\sum_C \Delta C E_C(\eta)}{\sum_C \Delta C} \quad , \tag{2}$$

is used as a global correction to obtain the primary charged-particle pseudorapidity density

$$\left.\frac{\mathrm{d}N_{ch}}{\mathrm{d}\eta}\right|_{X,\mathrm{primary}} = \frac{1}{E(\eta)} \left.\frac{\mathrm{d}N_{ch}}{\mathrm{d}\eta}\right|_{X,\mathrm{inclusive,nominal}} \quad , \tag{3}$$

where X stands for an event selection e.g., a centrality range.

The simulation-based correction $S(\eta)$ for secondary particles to the charged-particle pseudorapidity density in the forward directions is given by

$$S(\eta) = \frac{N_{\mathrm{inclusive,FMD}}(\eta)}{N_{\mathrm{primary,generated}}(\eta)} \quad , \tag{4}$$

where $N_{\mathrm{inclusive,FMD}}$ is the number of primary *and* secondary particles impinging on the FMD − as given by the track propagation of the simulation, and $N_{\mathrm{primary,generated}}$ is the number of generated primary particles at a given pseudorapidity. Complete detector-simulation studies show that three effects can contribute to the generation of secondaries, and hence the value of $S(\eta)$. These three effects are: material in which secondaries are produced, the transverse momentum (p_T) distribution and particle composition of the generated particles, and lastly the total number of produced particles. Of these three the material is by far the dominant effect, while the p_T and particle composition only effects $S(\eta)$ on the few percent level. The total number of generated particles has a negligible effect on $S(\eta)$. That is, the material surrounding the detectors amplifies the primary-particle signal through particle production by a constant factor that first and foremost depends on the amount of material itself, and only secondarily on the p_T and particle composition of the generated primary particles.

To estimate how much $E_C(\eta)$ itself would have changed if another system or centrality range was used to calculate the correction, $S(\eta)$ is analysed from simulations with various collision systems and energies. We find that, even for large variations in particle composition and p_T distributions, $S(\eta)$ only varies by up to 5%. Reweighting the particle composition and p_T distributions from the various systems to match produces consistent values of $S(\eta)$ ensuring that the 5% variations found were only due to particle composition and p_T distributions differences. This uncertainty is applied to $E(\eta)$ to account for all reasonable variations of the particle composition and p_T distributions, which cannot be measured in the forward regions of ALICE.

Fig. 1 shows the comparison of the data driven correction $E(\eta)$ to the simulation-based correction $S(\eta)$ from PYTHIA [15] (pp) and a parameterisation of the available ALICE results [16,17] for Pb–Pb collisions. The simulated collisions are for two distinct systems and span over almost an order of magnitude in collision energy. The total number of produced particles in these simulations span five orders of magnitude, and no dependence of $S(\eta)$ on charged-particle multiplicity is observed.

By comparing $E(\eta)$ to $S(\eta)$ from simulations, one finds a good correspondence between the two corrections *except* in regions

where the material description in the simulations is known to be inadequate. This, together with the fact that the numerator and denominator of Eq. (1) measure the same physical process, but differ foremost in the material traversed by the primary particles, and hence the number of secondary particles observed, implies that the correction $E(\eta)$ is universal. That is, Eq. (3) is applicable for *any* event selection X in any collision system or at any collision energy, where the produced multiplicity, p_T distributions, and particle composition is close to the range of the simulated systems used to study $S(\eta)$.

Note, for the previously published results [6], which used satellite–main collisions, the simulation-based approach for correcting for secondary particles i.e., applying $S(\eta)$ directly, was valid. As mentioned above, in satellite–main collisions, the particles that impinge on the FMD traverse far less and better described material in the simulation of the ALICE apparatus. The use of a simulation-based correction for secondary particles was in that analysis cross-checked by comparing to and combining with measurements from the V0 and SPD [6]. Despite concerted efforts to improve the simulations by the Collaboration it has not been possible to achieve the same accuracy in $S(\eta)$ for main–main collisions.

Finally, the effect of variation of the location of the primary interaction point on $E(\eta)$ was studied. It was found, that the effect is negligible, given that the distribution of IP_z are similar between the numerator of Eq. (1) and right-hand side of Eq. (3), as was the case in this analysis.

The method used in this analysis to extract the inclusive number of charged particles from the FMD is the same as for previous published results [6], *except* that the data-driven correction $E(\eta)$ − rather than a simulation-based one $S(\eta)$ − is used to correct for secondary particles.

4. Systematic uncertainties

Table 2 summarises the systematic uncertainties of this analysis. The common systematic uncertainty from the centrality selection is correlated across η and detailed elsewhere [13].

For the SPD measurements, the systematic uncertainties are the same as for the previously published mid-rapidity result [7], except for a contribution from the correction due to the larger acceptance used in this analysis. This uncertainty stems from the range of IP_z used in the analysis (here $|IP_z| < 15$ cm). At larger absolute values of IP_z the acceptance correction for the SPD tracklets grows, and the uncertainty with it, being therefore η-dependent and largest at $|\eta| \approx 2$.

The various sources of systematic uncertainties for the FMD measurements are detailed elsewhere [6], but will be expanded upon in the following since some values have changed due to better understanding of the detector response.

In the analysis, three η-dependent thresholds are used. The values for these thresholds are obtained by fitting a convoluted Landau–Gauss distribution [18] to the energy loss spectrum measured by the FMD in a given η range. The uncertainties associated with these thresholds are detailed below.

A charged particle traversing the FMD can deposit energy in more than one element i.e., strip, of the detector. Therefore it is necessary to recombine two signals to get the single charged-particle energy loss in those cases. This recombination depends on a lower threshold for accepting a signal, and an upper threshold to consider a signal as isolated i.e., all energy is deposited in a single strip. The systematic uncertainties from the recombination of signals are found by varying the lower and upper threshold values within bounds of the energy loss fits and by simulation studies.

To calculate the inclusive number of charged particles, a statistical approach is used [6]. The strips of the FMD are divided into

Table 2
Summary of systematic uncertainties: the common systematic uncertainties shared by both the SPD and the FMD, and the uncertainties particular to the detectors.

Detector	Source	Uncertainty (%)
Common	Centrality	0.4–6.2
SPD	Background subtraction	0.1
	Particle composition	1
	Weak decays	1
	Extrapolation to $p_T = 0$	2
	Event generator	2
	Acceptance	0–2[a]
FMD	Recombination	1
	Threshold	$^{+1}_{-2}$
	Secondary particles	6.1
	Particle composition & p_T	2[b]

[a] Pseudorapidity dependent uncertainty, largest at $|\eta| = 2$.
[b] Additional contribution in $3.7 < \eta < 5$. See also text.

regions, and the number of empty strips is compared to the total number of strips in a given region. Strips with a signal below a given threshold are considered empty. The threshold was varied within bounds of the energy loss fits and investigated in simulation studies to obtain the systematic uncertainty.

The data-driven correction for secondary particles defined in Eq. (2) is derived from the previously published results, and as such contains contributions from the systematic uncertainties of those results [6]. Factoring out common correlated uncertainties e.g., the contribution from the centrality determination, we find a contribution of 4.7% from the previously published results. By studying the variation of the numerator of Eq. (1) under different experimental conditions e.g., different data-taking periods, and adding the variance in quadrature, the uncorrelated, total uncertainty on $E(\eta)$ is found to be 6.1%. Systematic uncertainties can in general *not* be cancelled between the numerator and denominator of Eq. (1), since the same η regions are probed by different detector elements in each.

Note, that the previously published result [6] used in Eq. (1) already carries a 2% systematic uncertainty from the particle composition and p_T distribution [6]. This contribution is contained in the 4.7% quoted above, and is propagated to the final 6.1% systematic uncertainty on $E(\eta)$.

Finally, it was found through simulations that the acceptance region of FMD1 is particularly affected by the variations in the number of secondary particles stemming from variations in the particle composition and p_T distribution, and gives rise to an additional 2% systematic uncertainty, which is added in quadrature to the rest of the systematic uncertainties, but only for $\eta > 3.7$.

5. Results

Fig. 2 shows the charged-particle pseudorapidity density for different centralities from each detector separately.

The combined distributions in Fig. 3 are calculated as the average of the individual measurements from the FMD and SPD, weighted by statistical errors and systematic uncertainties, omitting those which are common such as that from the centrality determination. The distributions are then symmetrised around $\eta = 0$ by taking the weighted average of $\pm\eta$ points. Points at $3.5 < \eta < 5$ are reflected on to $-5 < \eta < -3.5$ to provide the $dN_{ch}/d\eta$ distributions in a range comparable to the previously published results [6].

The lines in Fig. 3 are fits of

$$f_{GG}(\eta; A_1, \sigma_1, A_2, \sigma_2) = A_1 e^{-\frac{1}{2}\frac{\eta^2}{\sigma_1^2}} - A_2 e^{-\frac{1}{2}\frac{\eta^2}{\sigma_2^2}} , \qquad (5)$$
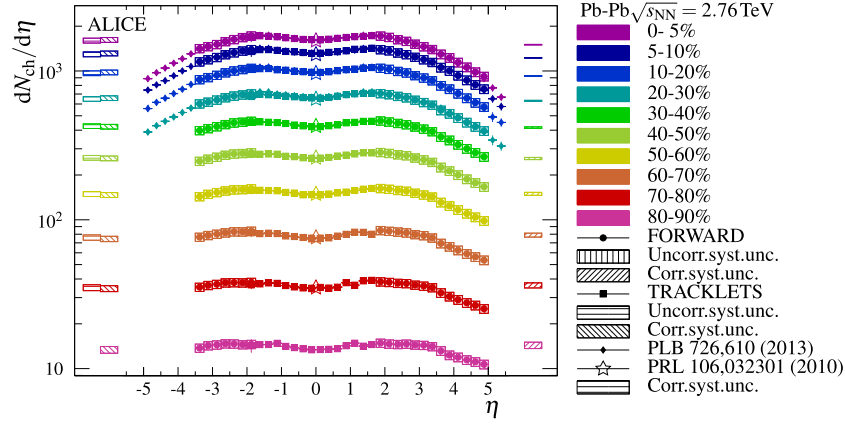
Fig. 2. (Colour online.) Measurement of $dN_{ch}/d\eta$ per centrality from SPD (squares) and FMD (circles) separately. Error bars reflect the total uncorrelated systematic uncertainty and statistical error on each point. Error bars on the left and right reflect the correlated systematic uncertainties on the SPD and FMD points, respectively. Previously published results for 0–30% over the full pseudorapidity range (diamonds) [6] and for 0–80% at mid-rapidity (stars) [7] are also shown.
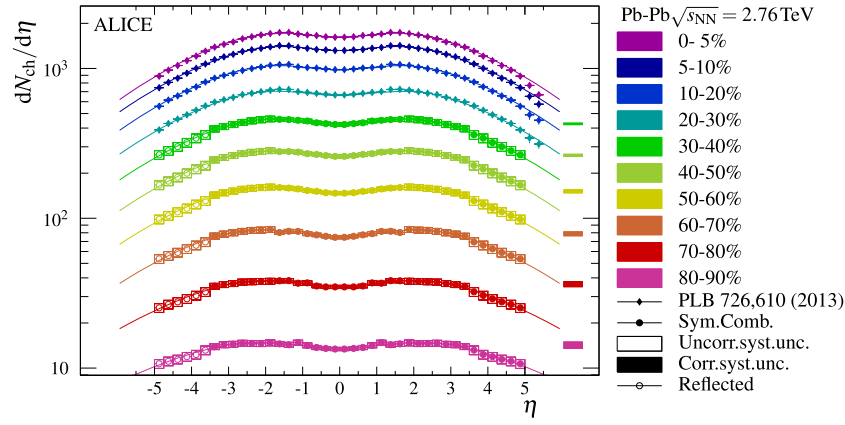
Fig. 3. (Colour online.) Measurement of $dN_{ch}/d\eta$ for all centralities and a broad η range. Combined and symmetrised $dN_{ch}/d\eta$ over 30–90% centrality from both SPD and FMD (circles). Open boxes reflect the total uncorrelated systematic uncertainties and statistical errors, while the filled boxes on the right reflect the correlated systematic uncertainty. Also shown, is the reflection of the $3.5 < \eta < 5$ values around $\eta = 0$ (open circles). Previously published results for 0–30% over the full pseudorapidity range (diamonds) [6] are also shown. The lines correspond to fits of Eq. (5) to the data.

to the measured distributions. The function f_{GG} is the difference of two Gaussian distributions centred at $\eta = 0$ with amplitudes A_1, A_2, and widths σ_1, σ_2. The function describes the data well within the measured region with a reduced χ^2 smaller than 1. We find values of A_2/A_1 for all centralities, from 0.20 to 0.31 but are consistent within fit uncertainties, with a constant value of 0.23 ± 0.02. Likewise values of σ_2/σ_1 for all centralities, ranges from 0.28 to 0.36 and are consistent with a constant value of 0.31 ± 0.02.

Qualitatively the shape of the charged-particle pseudorapidity density distributions broadens only slightly toward more peripheral events, consistent with the above observation. Indeed, the full-width half-maximum (FWHM) shown in Fig. 4 versus the number of participating nucleons $\langle N_{part} \rangle$ — calculated using a Glauber model [13] — increase sharply only in the very most peripheral collisions. The $dN_{ch}/d\eta$ distributions does not extend far enough to calculate reliable values for FWHM directly from the data. Instead $f_{GG}(\eta) - \max(f_{GG})/2 = 0$ was numerically solved, and the uncertainties evaluated as the error of f_{GG} at the roots, divided by the slope at those roots. The width of the $dN_{ch}/d\eta$ distributions follows the same trend, in the region of 0–50%, as was seen in lower energy results from PHOBOS reproduced in Fig. 4 for comparison [2].

Fig. 5 presents the charged-particle pseudorapidity density per average number of participating nucleon pairs $\langle N_{part} \rangle/2$ as a function of the average number of participants $\langle N_{part} \rangle$. Although there

is a slight increase in the ratio to the central pseudorapidity density distribution at low $\langle N_{part} \rangle$ (see lower part of Fig. 5), the uncertainties are large and no strong evolution of the shape of the pseudorapidity density distribution over pseudorapidity with respect to centrality is observed. The ratio at $3.5 < |\eta| < 4.5$ does deviate somewhat in peripheral collisions, which is attributed to the general broadening of the pseudorapidity density distributions in those collisions.

To extract the total number of charged particles produced in Pb–Pb collisions at various centralities, a number of functions, including Eq. (5), is fitted to the $dN_{ch}/d\eta$ distributions. A trapezoid

$$
f_{T}(\eta; y_{beam}, M, A) = A \times \begin{cases} 0 & |\eta| > y_{beam} \\ (y_{beam} + \eta) & \eta < -M \\ (y_{beam} - M) & |\eta| < M \\ (y_{beam} - \eta) & \eta > +M, \end{cases} \quad (6)
$$

was successfully used by PHOBOS to describe limiting fragmentation [2]. Here, $[-M, M]$ is the range in which the function is constant, and A is the amplitude. The parameterisation

$$
f_{P}(\eta; A, \alpha, \beta, a) = A \frac{\sqrt{1 - 1/[\alpha \cosh(\eta)]^2}}{1 + e^{(|\eta| - \beta)/a}} \quad , \quad (7)
$$

as suggested by PHOBOS, is likewise fitted to the $dN_{ch}/d\eta$ distributions. The parameter a expresses the width of the distribution, and
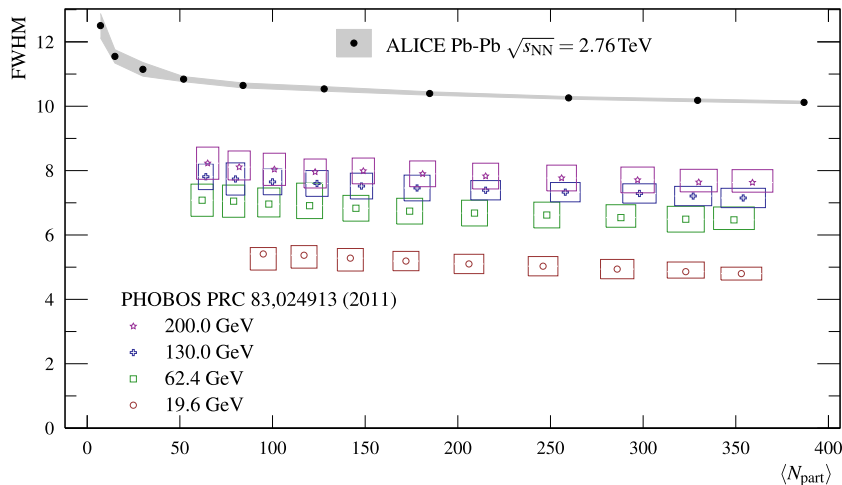
Fig. 4. (Colour online.) Full-width half-maximum of the charged-particle pseudorapidity distributions versus the average number of participants. The uncertainties on the ALICE measurements are from the fit of f_{GG} only and evaluated at 95% confidence level. Also shown are lower energy results from PHOBOS [2].
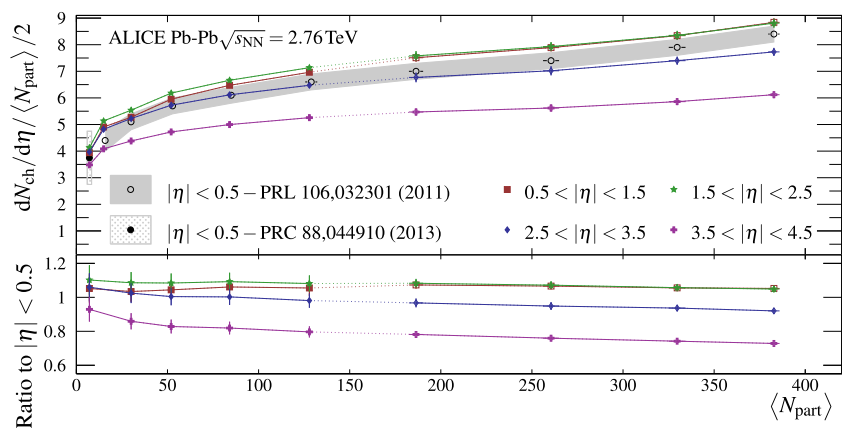
Fig. 5. (Colour online.) The charged-particle pseudorapidity density distributions scaled by the average number of participants in various pseudorapidity intervals as a function of the number of participants. The four right-most points (open symbols) in each η range, as well as the mid-rapidity points (circles) are from previously published results [6, 17]. The uncertainties on $\langle N_{part} \rangle$ from the Glauber calculations are only included on the points at mid-rapidity. Thus, the uncertainty band around the mid-rapidity points reflect both the measurement uncertainties and the uncertainty on $\langle N_{part} \rangle$, while other η ranges only show the measurement uncertainties. The lower part shows the ratio of each distribution to the previously published distributions for $|\eta| < 0.5$.

α and β, and expresses the width and depth of the dip at $\eta \approx 0$, respectively. A is an overall scale parameter. Finally, to remedy some of the obvious defects of the trapezoid i.e., a non-continuous first derivative at $\eta = M$, we use a Bjorken-inspired function [6]

$$f_B(\eta; A, \mu, \sigma) = A \times \begin{cases} e^{-\frac{(\eta+\mu)^2}{2\sigma^2}} & \eta < -\mu \\ e^{-\frac{(\eta-\mu)^2}{2\sigma^2}} & \eta > +\mu \\ 1 & |\eta| < \mu, \end{cases} \qquad (8)$$

which has plateau at A for $|\eta| < \mu$ connected to Gaussian fall-off beyond $\pm\mu$. The fitted functions are integrated over η up to the beam rapidity $\pm y_{beam} = \pm 7.99$. Although the $dN_{ch}/d\eta$ distributions in principle continue to infinity, there is no significant loss in generality or precision by cutting the integral at $\eta = \pm y_{beam}$ since the distributions rapidly approach zero. Notice that all parameters of the functions are left free in the fitting procedure. All functions give reasonable fits (with a reduced χ^2 smaller than 1), though the trapezoid and Bjorken-inspired ansatz are too flat at the mid-rapidity. The calculation of the central values and uncertainties are done as for previous results [6]: The central value is calculated from the integral of the trapezoid fit to compare directly to previ-

ous results; the spread between the integrals and the central value is evaluated to obtain the uncertainty on the total N_{ch}.

The extrapolated total N_{ch} versus $\langle N_{part} \rangle$ is shown in Fig. 6, and compared to lower energy results from PHOBOS [19]. At LHC energies the particle production as a function of $\langle N_{part} \rangle$ shows a similar behaviour to the lower energy results, and the factorisation [2] in centrality and energy seems to hold (see fit in Fig. 6).

In Fig. 7 we show comparisons of various model calculations to the measured charged-particle pseudorapidity density as a function of centrality. The centrality class for a given model-generated event was determined by sharp cuts in the impact parameter b and a Glauber calculation [13].

The HIJING model [3] (version 1.383, with jet-quenching disabled, shadowing enabled, and a hard p_T cut-off of 2.3 GeV) is seen to overshoot the data for all centralities. In addition, the distributions at all centralities decrease with increasing $|\eta|$ faster than the data would suggest.

AMPT [4] without string melting reproduces the data fairly well at central pseudorapidity for the most central events — exactly in the region it was tuned to, but it fails to describe the charged-particle pseudorapidity density for more peripheral events. Also, AMPT without string melting would suggest a wider central region than supported by data, and similarly to HIJING decreases
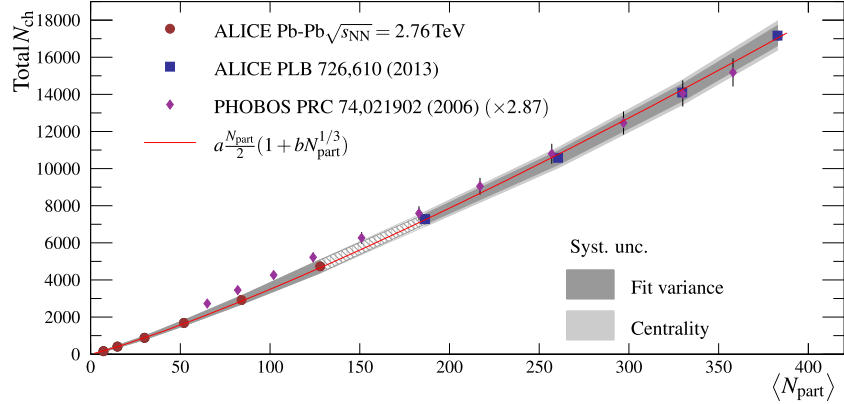
Fig. 6. (Colour online.) Extrapolation to the total number of charged particles as a function of the number of participating nucleons [13]. The uncertainty on the extrapolation is smaller than the size of the markers. The four right–most points are the previously published results [6]. A function inspired by factorisation [2] is fitted to the data, and the best fit yield $a = 35.8 \pm 4.2$, $b = 0.22 \pm 0.05$ with a reduced χ^2 of 0.18. Also shown is the PHOBOS result at lower energy result [19] scaled to the ALICE total number of charged particles per participant at $\langle N_{\text{part}} \rangle = 180$.
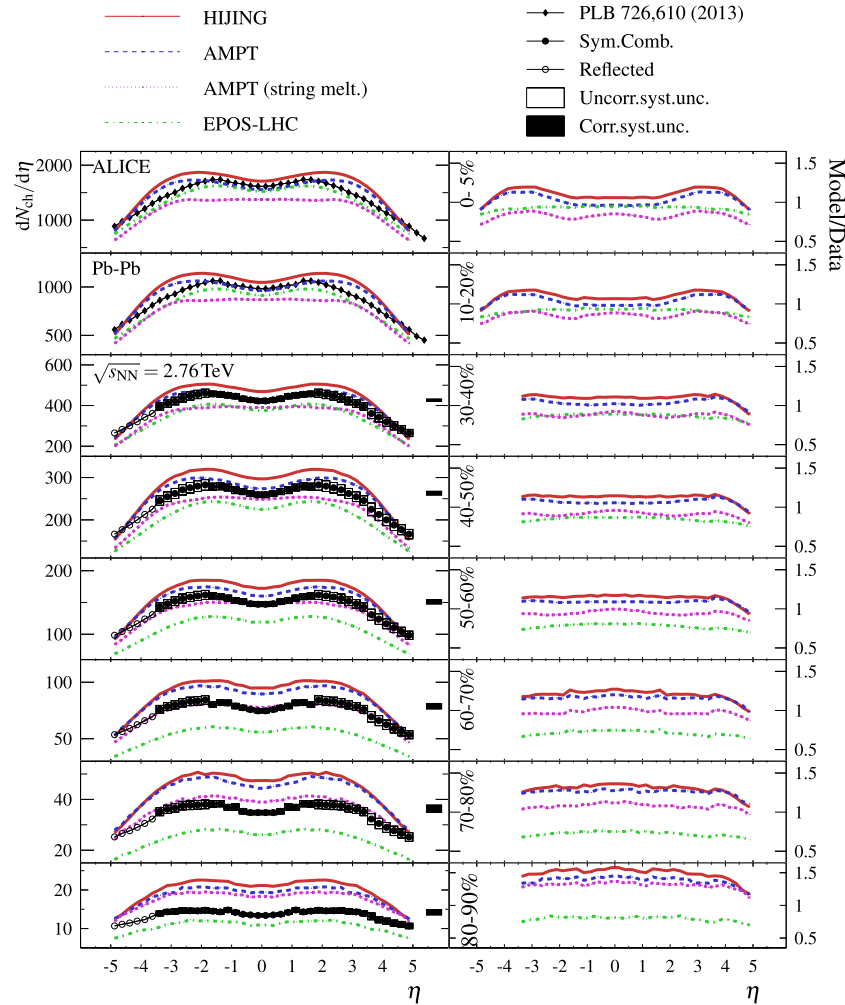
Fig. 7. (Colour online.) Comparison of $dN_{\text{ch}}/d\eta$ per centrality class from HIJING, AMPT (with and without string melting), and EPOS-LHC model calculations to the measured distributions.

faster than the data. AMPT with string melting — which essentially implements quark coalescence, and therefore a more predominant parton phase — is seen to be very flat at mid-rapidity and under-estimates the yield, except for peripheral collisions.

Finally, EPOS–LHC [5] reproduces the shape fairly well, but un-derestimates the data by 10 to 30%.

6. Conclusions

The charged-particle pseudorapidity density has been measured in Pb–Pb collisions at $\sqrt{s_{\text{NN}}} = 2.76$ TeV over a broad pseudo-rapidity range, extending previous published results by ALICE to more peripheral collisions. In the mid-rapidity region the well-

established tracklet procedure was used. In the forward regions, a new data-driven procedure to correct for the large background due to secondary particles was used. The results presented here are consistent with the behaviour previously seen in more central collisions and in a limited pseudorapidity range. No strong evolution of the overall shape of the charged-particle pseudorapidity density distributions as a function of collision centrality is observed. When normalised to the number of participating nucleons in the collision, the centrality evolution is small over the pseudorapidity range. Since the measurement was performed over a large pseudorapidity range ($-3.5 < \eta < 5$), it allows for an estimate of the total number of charged particles produced in Pb–Pb collisions at $\sqrt{s_{NN}} = 2.76$ TeV. The total charged-particle multiplicity is found to scale approximately with the number of participating nucleons. This would suggest that hard contributions to the total charged-particle multiplicity are small. From peripheral to central collisions we observe an increase of two orders of magnitude in the number of produced charge particles. A comparison of the data to the different available predictions from HIJING, AMPT, and EPOS-LHC show that none of these models captures both the shape and level of the measured distributions. AMPT however comes close in limited ranges of centrality. The exact centrality ranges that AMPT describes depend strongly on whether string melting is used in the model or not. EPOS-LHC — although systematically low — shows a reasonable agreement with the shape of the measured charged-particle pseudorapidity density distribution over a wider pseudorapidity range.

Acknowledgements

References

[1] L. Gribov, E. Levin, M. Ryskin, Semihard processes in QCD, Phys. Rep. 100 (1983) 1–150.

[2] PHOBOS Collaboration, B. Alver, et al., Charged-particle multiplicity and pseudorapidity distributions measured with the PHOBOS detector in Au+Au, Cu+Cu, d+Au, p+p collisions at ultrarelativistic energies, Phys. Rev. C 83 (2011) 024913.

[3] X.-N. Wang, M. Gyulassy, HIJING: a Monte Carlo model for multiple jet production in pp, pA and AA collisions, Phys. Rev. D 44 (1991) 3501–3516.

[4] Z.-W. Lin, C.M. Ko, B.-A. Li, B. Zhang, S. Pal, A multi-phase transport model for relativistic heavy ion collisions, Phys. Rev. C 72 (2005) 064901, arXiv:nucl-th/0411110.

[5] T. Pierog, I. Karpenko, J.M. Katzy, E. Yatsenko, K. Werner, EPOS LHC: test of collective hadronization with data measured at the CERN Large Hadron Collider, Phys. Rev. C 92 (3) (2015) 034906, arXiv:1306.0121 [hep-ph].

[6] ALICE Collaboration, E. Abbas, et al., Centrality dependence of the pseudorapidity density distribution for charged particles in Pb–Pb collisions at $\sqrt{s_{NN}} = 2.76$ TeV, Phys. Lett. B 726 (2013) 610–622, arXiv:1304.0347 [nucl-ex].

[7] ALICE Collaboration, K. Aamodt, et al., Centrality dependence of the charged-particle multiplicity density at mid-rapidity in Pb–Pb collisions at $\sqrt{s_{NN}} = 2.76$ TeV, Phys. Rev. Lett. 106 (2011) 032301, arXiv:1012.1657 [nucl-ex].

[8] ATLAS Collaboration, G. Aad, et al., Measurement of the centrality dependence of the charged particle pseudorapidity distribution in lead–lead collisions at $\sqrt{s_{NN}} = 2.76$ TeV with the ATLAS detector, Phys. Lett. B 710 (2012) 363–382, arXiv:1108.6027 [hep-ex].

[9] CMS Collaboration, S. Chatrchyan, et al., Dependence on pseudorapidity and centrality of charged hadron production in PbPb collisions at a nucleon–nucleon centre-of-mass energy of 2.76 TeV, J. High Energy Phys. 08 (2011) 141, arXiv:1107.4800 [nucl-ex].

[10] ALICE Collaboration, K. Aamodt, et al., The ALICE experiment at the CERN LHC, J. Instrum. 3 (2008) S08002.

[11] ALICE Collaboration, B. Abelev, et al., Performance of the ALICE experiment at the CERN LHC, Int. J. Mod. Phys. A 29 (2014) 1430044, arXiv:1402.4476 [nucl-ex].

[12] ALICE Collaboration, K. Aamodt, et al., Charged-particle multiplicity density at mid-rapidity in central Pb–Pb collisions at $\sqrt{s_{NN}} = 2.76$ TeV, Phys. Rev. Lett. 105 (2010) 252301, arXiv:1011.3916 [nucl-ex].

[13] ALICE Collaboration, B. Abelev, et al., Centrality determination of Pb–Pb collisions at $\sqrt{s_{NN}} = 2.76$ TeV with ALICE, Phys. Rev. C 88 (2013) 044909, arXiv:1301.4361 [nucl-ex].

[14] C.P. Welsch, et al., Measurement of satellite bunches at the LHC, Conf. Proc. C 1205201 (2012) 97–99.

[15] T. Sjostrand, S. Mrenna, P.Z. Skands, PYTHIA 6.4 physics and manual, J. High Energy Phys. 05 (2006) 026, arXiv:hep-ph/0603175.

[16] ALICE Collaboration, B. Abelev, et al., Elliptic flow of identified hadrons in Pb–Pb collisions at $\sqrt{s_{NN}} = 2.76$ TeV, J. High Energy Phys. 06 (2015) 190, arXiv:1405.4632 [nucl-ex].

[17] ALICE Collaboration, B. Abelev, et al., Centrality dependence of π, K, p production in Pb–Pb collisions at $\sqrt{s_{NN}} = 2.76$ TeV, Phys. Rev. C 88 (2013) 044910, arXiv:1303.0737 [hep-ex].

[18] S. Hancock, F. James, J. Movchet, P.G. Rancoita, L. Van Rossum, Energy loss distributions for single particles and several particles in a thin silicon absorber, Nucl. Instrum. Methods B 1 (1984) 16.

[19] PHOBOS Collaboration, B. Alver, et al., Scaling properties in bulk and $p(T)$-dependent particle production near midrapidity in relativistic heavy ion collisions, Phys. Rev. C 80 (2009) 011901, arXiv:0808.1895 [nucl-ex].

ALICE Collaboration

J. Adam [40], D. Adamová [83], M.M. Aggarwal [87], G. Aglieri Rinella [36], M. Agnello [110], N. Agrawal [48], Z. Ahammed [132], S.U. Ahn [68], S. Aiola [136], A. Akindinov [58], S.N. Alam [132], D. Aleksandrov [99], B. Alessandro [110], D. Alexandre [101], R. Alfaro Molina [64], A. Alici [12,104], A. Alkin [3], J.R.M. Almaraz [119], J. Alme [38], T. Alt [43], S. Altinpinar [18], I. Altsybeev [131], C. Alves Garcia Prado [120], C. Andrei [78], A. Andronic [96], V. Anguelov [93], J. Anielski [54], T. Antičić [97], F. Antinori [107], P. Antonioli [104], L. Aphecetche [113], H. Appelshäuser [53], S. Arcelli [28], R. Arnaldi [110], O.W. Arnold [37,92], I.C. Arsene [22], M. Arslandok [53], B. Audurier [113], A. Augustinus [36], R. Averbeck [96], M.D. Azmi [19], A. Badalà [106], Y.W. Baek [67,44], S. Bagnasco [110], R. Bailhache [53], R. Bala [90], A. Baldisseri [15], R.C. Baral [61], A.M. Barbano [27], R. Barbera [29], F. Barile [33], G.G. Barnaföldi [135], L.S. Barnby [101], V. Barret [70], P. Bartalini [7], K. Barth [36], J. Bartke [117], E. Bartsch [53], M. Basile [28], N. Bastid [70], S. Basu [132], B. Bathen [54], G. Batigne [113], A. Batista Camejo [70], B. Batyunya [66], P.C. Batzing [22], I.G. Bearden [80], H. Beck [53], C. Bedda [110], N.K. Behera [50], I. Belikov [55], F. Bellini [28], H. Bello Martinez [2], R. Bellwied [122], R. Belmont [134], E. Belmont-Moreno [64], V. Belyaev [75], G. Bencedi [135], S. Beole [27], I. Berceanu [78], A. Bercuci [78], Y. Berdnikov [85], D. Berenyi [135], R.A. Bertens [57], D. Berzano [36], L. Betev [36], A. Bhasin [90], I.R. Bhat [90], A.K. Bhati [87], B. Bhattacharjee [45], J. Bhom [128], L. Bianchi [122], N. Bianchi [72], C. Bianchin [57,134], J. Bielčík [40], J. Bielčíková [83], A. Bilandzic [80], R. Biswas [4], S. Biswas [79], S. Bjelogrlic [57], J.T. Blair [118], D. Blau [99], C. Blume [53], F. Bock [93,74], A. Bogdanov [75], H. Bøggild [80], L. Boldizsár [135], M. Bombara [41], J. Book [53], H. Borel [15], A. Borissov [95], M. Borri [82,124], F. Bossú [65], E. Botta [27], S. Böttger [52], C. Bourjau [80], P. Braun-Munzinger [96], M. Bregant [120], T. Breitner [52], T.A. Broker [53], T.A. Browning [94], M. Broz [40], E.J. Brucken [46], E. Bruna [110], G.E. Bruno [33], D. Budnikov [98], H. Buesching [53], S. Bufalino [27,36], P. Buncic [36], O. Busch [93,128], Z. Buthelezi [65], J.B. Butt [16], J.T. Buxton [20], D. Caffarri [36], X. Cai [7], H. Caines [136], L. Calero Diaz [72], A. Caliva [57], E. Calvo Villar [102], P. Camerini [26], F. Carena [36], W. Carena [36], F. Carnesecchi [28], J. Castillo Castellanos [15], A.J. Castro [125], E.A.R. Casula [25], C. Ceballos Sanchez [9], J. Cepila [40], P. Cerello [110], J. Cerkala [115], B. Chang [123], S. Chapeland [36], M. Chartier [124], J.L. Charvet [15], S. Chattopadhyay [132], S. Chattopadhyay [100], V. Chelnokov [3], M. Cherney [86], C. Cheshkov [130], B. Cheynis [130], V. Chibante Barroso [36], D.D. Chinellato [121], S. Cho [50], P. Chochula [36], K. Choi [95], M. Chojnacki [80], S. Choudhury [132], P. Christakoglou [81], C.H. Christensen [80], P. Christiansen [34], T. Chujo [128], S.U. Chung [95], C. Cicalo [105], L. Cifarelli [12,28], F. Cindolo [104], J. Cleymans [89], F. Colamaria [33], D. Colella [59,33,36], A. Collu [74,25], M. Colocci [28], G. Conesa Balbastre [71], Z. Conesa del Valle [51], M.E. Connors [136,ii], J.G. Contreras [40], T.M. Cormier [84], Y. Corrales Morales [110], I. Cortés Maldonado [2], P. Cortese [32], M.R. Cosentino [120], F. Costa [36], P. Crochet [70], R. Cruz Albino [11], E. Cuautle [63], L. Cunqueiro [36], T. Dahms [92,37], A. Dainese [107], A. Danu [62], D. Das [100], I. Das [51,100], S. Das [4], A. Dash [121,79], S. Dash [48], S. De [120], A. De Caro [31,12], G. de Cataldo [103], C. de Conti [120], J. de Cuveland [43], A. De Falco [25], D. De Gruttola [12,31], N. De Marco [110], S. De Pasquale [31], A. Deisting [96,93], A. Deloff [77], E. Dénes [135,i], C. Deplano [81], P. Dhankher [48], D. Di Bari [33], A. Di Mauro [36], P. Di Nezza [72], M.A. Diaz Corchero [10], T. Dietel [89], P. Dillenseger [53], R. Divià [36], Ø. Djuvsland [18], A. Dobrin [57,81], D. Domenicis Gimenez [120], B. Dönigus [53], O. Dordic [22], T. Drozhzhova [53], A.K. Dubey [132], A. Dubla [57], L. Ducroux [130], P. Dupieux [70], R.J. Ehlers [136], D. Elia [103], H. Engel [52], E. Epple [136], B. Erazmus [113], I. Erdemir [53], F. Erhardt [129], B. Espagnon [51], M. Estienne [113], S. Esumi [128], J. Eum [95], D. Evans [101], S. Evdokimov [111], G. Eyyubova [40], L. Fabbietti [92,37], D. Fabris [107], J. Faivre [71], A. Fantoni [72], M. Fasel [74], L. Feldkamp [54], A. Feliciello [110], G. Feofilov [131], J. Ferencei [83], A. Fernández Téllez [2], E.G. Ferreiro [17], A. Ferretti [27], A. Festanti [30], V.J.G. Feuillard [15,70], J. Figiel [117], M.A.S. Figueredo [124,120], S. Filchagin [98], D. Finogeev [56], F.M. Fionda [25], E.M. Fiore [33], M.G. Fleck [93], M. Floris [36], S. Foertsch [65], P. Foka [96], S. Fokin [99], E. Fragiacomo [109], A. Francescon [30,36], U. Frankenfeld [96], U. Fuchs [36], C. Furget [71], A. Furs [56], M. Fusco Girard [31], J.J. Gaardhøje [80], M. Gagliardi [27], A.M. Gago [102], M. Gallio [27], D.R. Gangadharan [74], P. Ganoti [36,88], C. Gao [7], C. Garabatos [96], E. Garcia-Solis [13], C. Gargiulo [36], P. Gasik [37,92], E.F. Gauger [118], M. Germain [113],

A. Gheata [36], M. Gheata [62,36], P. Ghosh [132], S.K. Ghosh [4], P. Gianotti [72], P. Giubellino [36,110], P. Giubilato [30], E. Gladysz-Dziadus [117], P. Glässel [93], D.M. Gómez Coral [64], A. Gomez Ramirez [52], V. Gonzalez [10], P. González-Zamora [10], S. Gorbunov [43], L. Görlich [117], S. Gotovac [116], V. Grabski [64], O.A. Grachov [136], L.K. Graczykowski [133], K.L. Graham [101], A. Grelli [57], A. Grigoras [36], C. Grigoras [36], V. Grigoriev [75], A. Grigoryan [1], S. Grigoryan [66], B. Grinyov [3], N. Grion [109], J.M. Gronefeld [96], J.F. Grosse-Oetringhaus [36], J.-Y. Grossiord [130], R. Grosso [96], F. Guber [56], R. Guernane [71], B. Guerzoni [28], K. Gulbrandsen [80], T. Gunji [127], A. Gupta [90], R. Gupta [90], R. Haake [54], Ø. Haaland [18], C. Hadjidakis [51], M. Haiduc [62], H. Hamagaki [127], G. Hamar [135], J.W. Harris [136], A. Harton [13], D. Hatzifotiadou [104], S. Hayashi [127], S.T. Heckel [53], M. Heide [54], H. Helstrup [38], A. Herghelegiu [78], G. Herrera Corral [11], B.A. Hess [35], K.F. Hetland [38], H. Hillemanns [36], B. Hippolyte [55], R. Hosokawa [128], P. Hristov [36], M. Huang [18], T.J. Humanic [20], N. Hussain [45], T. Hussain [19], D. Hutter [43], D.S. Hwang [21], R. Ilkaev [98], M. Inaba [128], M. Ippolitov [75,99], M. Irfan [19], M. Ivanov [96], V. Ivanov [85], V. Izucheev [111], P.M. Jacobs [74], M.B. Jadhav [48], S. Jadlovska [115], J. Jadlovsky [115,59], C. Jahnke [120], M.J. Jakubowska [133], H.J. Jang [68], M.A. Janik [133], P.H.S.Y. Jayarathna [122], C. Jena [30], S. Jena [122], R.T. Jimenez Bustamante [96], P.G. Jones [101], H. Jung [44], A. Jusko [101], P. Kalinak [59], A. Kalweit [36], J. Kamin [53], J.H. Kang [137], V. Kaplin [75], S. Kar [132], A. Karasu Uysal [69], O. Karavichev [56], T. Karavicheva [56], L. Karayan [93,96], E. Karpechev [56], U. Kebschull [52], R. Keidel [138], D.L.D. Keijdener [57], M. Keil [36], M. Mohisin Khan [19], P. Khan [100], S.A. Khan [132], A. Khanzadeev [85], Y. Kharlov [111], B. Kileng [38], D.W. Kim [44], D.J. Kim [123], D. Kim [137], H. Kim [137], J.S. Kim [44], M. Kim [44], M. Kim [137], S. Kim [21], T. Kim [137], S. Kirsch [43], I. Kisel [43], S. Kiselev [58], A. Kisiel [133], G. Kiss [135], J.L. Klay [6], C. Klein [53], J. Klein [36,93], C. Klein-Bösing [54], S. Klewin [93], A. Kluge [36], M.L. Knichel [93], A.G. Knospe [118], T. Kobayashi [128], C. Kobdaj [114], M. Kofarago [36], T. Kollegger [96,43], A. Kolojvari [131], V. Kondratiev [131], N. Kondratyeva [75], E. Kondratyuk [111], A. Konevskikh [56], M. Kopcik [115], M. Kour [90], C. Kouzinopoulos [36], O. Kovalenko [77], V. Kovalenko [131], M. Kowalski [117], G. Koyithatta Meethaleveedu [48], I. Králik [59], A. Kravčáková [41], M. Kretz [43], M. Krivda [101,59], F. Krizek [83], E. Kryshen [36], M. Krzewicki [43], A.M. Kubera [20], V. Kučera [83], C. Kuhn [55], P.G. Kuijer [81], A. Kumar [90], J. Kumar [48], L. Kumar [87], S. Kumar [48], P. Kurashvili [77], A. Kurepin [56], A.B. Kurepin [56], A. Kuryakin [98], M.J. Kweon [50], Y. Kwon [137], S.L. La Pointe [110], P. La Rocca [29], P. Ladron de Guevara [11], C. Lagana Fernandes [120], I. Lakomov [36], R. Langoy [42], C. Lara [52], A. Lardeux [15], A. Lattuca [27], E. Laudi [36], R. Lea [26], L. Leardini [93], G.R. Lee [101], S. Lee [137], F. Lehas [81], R.C. Lemmon [82], V. Lenti [103], E. Leogrande [57], I. León Monzón [119], H. León Vargas [64], M. Leoncino [27], P. Lévai [135], S. Li [70,7], X. Li [14], J. Lien [42], R. Lietava [101], S. Lindal [22], V. Lindenstruth [43], C. Lippmann [96], M.A. Lisa [20], H.M. Ljunggren [34], D.F. Lodato [57], P.I. Loenne [18], V. Loginov [75], C. Loizides [74], X. Lopez [70], E. López Torres [9], A. Lowe [135], P. Luettig [53], M. Lunardon [30], G. Luparello [26], A. Maevskaya [56], M. Mager [36], S. Mahajan [90], S.M. Mahmood [22], A. Maire [55], R.D. Majka [136], M. Malaev [85], I. Maldonado Cervantes [63], L. Malinina [66,iii], D. Mal'Kevich [58], P. Malzacher [96], A. Mamonov [98], V. Manko [99], F. Manso [70], V. Manzari [36,103], M. Marchisone [27,65,126], J. Mareš [60], G.V. Margagliotti [26], A. Margotti [104], J. Margutti [57], A. Marín [96], C. Markert [118], M. Marquard [53], N.A. Martin [96], J. Martin Blanco [113], P. Martinengo [36], M.I. Martínez [2], G. Martínez García [113], M. Martinez Pedreira [36], A. Mas [120], S. Masciocchi [96], M. Masera [27], A. Masoni [105], L. Massacrier [113], A. Mastroserio [33], A. Matyja [117], C. Mayer [117], J. Mazer [125], M.A. Mazzoni [108], D. Mcdonald [122], F. Meddi [24], Y. Melikyan [75], A. Menchaca-Rocha [64], E. Meninno [31], J. Mercado Pérez [93], M. Meres [39], Y. Miake [128], M.M. Mieskolainen [46], K. Mikhaylov [66,58], L. Milano [36], J. Milosevic [22], L.M. Minervini [103,23], A. Mischke [57], A.N. Mishra [49], D. Miśkowiec [96], J. Mitra [132], C.M. Mitu [62], N. Mohammadi [57], B. Mohanty [79,132], L. Molnar [55,113], L. Montaño Zetina [11], E. Montes [10], D.A. Moreira De Godoy [54,113], L.A.P. Moreno [2], S. Moretto [30], A. Morreale [113], A. Morsch [36], V. Muccifora [72], E. Mudnic [116], D. Mühlheim [54], S. Muhuri [132], M. Mukherjee [132], J.D. Mulligan [136], M.G. Munhoz [120], R.H. Munzer [92,37], S. Murray [65], L. Musa [36], J. Musinsky [59], B. Naik [48], R. Nair [77], B.K. Nandi [48], R. Nania [104], E. Nappi [103], M.U. Naru [16], H. Natal da Luz [120], C. Nattrass [125], K. Nayak [79], T.K. Nayak [132], S. Nazarenko [98], A. Nedosekin [58], L. Nellen [63], F. Ng [122], M. Nicassio [96], M. Niculescu [62], J. Niedziela [36], B.S. Nielsen [80], S. Nikolaev [99], S. Nikulin [99], V. Nikulin [85], F. Noferini [12,104], P. Nomokonov [66], G. Nooren [57], J.C.C. Noris [2], J. Norman [124], A. Nyanin [99], J. Nystrand [18], H. Oeschler [93], S. Oh [136], S.K. Oh [67], A. Ohlson [36], A. Okatan [69], T. Okubo [47], L. Olah [135], J. Oleniacz [133], A.C. Oliveira Da Silva [120], M.H. Oliver [136], J. Onderwaater [96], C. Oppedisano [110], R. Orava [46], A. Ortiz Velasquez [63], A. Oskarsson [34], J. Otwinowski [117], K. Oyama [93,76], M. Ozdemir [53], Y. Pachmayer [93], P. Pagano [31], G. Paić [63], S.K. Pal [132], J. Pan [134], A.K. Pandey [48],

P. Papcun [115], V. Papikyan [1], G.S. Pappalardo [106], P. Pareek [49], W.J. Park [96], S. Parmar [87], A. Passfeld [54], V. Paticchio [103], R.N. Patra [132], B. Paul [100], T. Peitzmann [57], H. Pereira Da Costa [15], E. Pereira De Oliveira Filho [120], D. Peresunko [99,75], C.E. Pérez Lara [81], E. Perez Lezama [53], V. Peskov [53], Y. Pestov [5], V. Petráček [40], V. Petrov [111], M. Petrovici [78], C. Petta [29], S. Piano [109], M. Pikna [39], P. Pillot [113], O. Pinazza [104,36], L. Pinsky [122], D.B. Piyarathna [122], M. Płoskoń [74], M. Planinic [129], J. Pluta [133], S. Pochybova [135], P.L.M. Podesta-Lerma [119], M.G. Poghosyan [84,86], B. Polichtchouk [111], N. Poljak [129], W. Poonsawat [114], A. Pop [78], S. Porteboeuf-Houssais [70], J. Porter [74], J. Pospisil [83], S.K. Prasad [4], R. Preghenella [36,104], F. Prino [110], C.A. Pruneau [134], I. Pshenichnov [56], M. Puccio [27], G. Puddu [25], P. Pujahari [134], V. Punin [98], J. Putschke [134], H. Qvigstad [22], A. Rachevski [109], S. Raha [4], S. Rajput [90], J. Rak [123], A. Rakotozafindrabe [15], L. Ramello [32], F. Rami [55], R. Raniwala [91], S. Raniwala [91], S.S. Räsänen [46], B.T. Rascanu [53], D. Rathee [87], K.F. Read [125,84], K. Redlich [77], R.J. Reed [134], A. Rehman [18], P. Reichelt [53], F. Reidt [93,36], X. Ren [7], R. Renfordt [53], A.R. Reolon [72], A. Reshetin [56], J.-P. Revol [12], K. Reygers [93], V. Riabov [85], R.A. Ricci [73], T. Richert [34], M. Richter [22], P. Riedler [36], W. Riegler [36], F. Riggi [29], C. Ristea [62], E. Rocco [57], M. Rodríguez Cahuantzi [2,11], A. Rodriguez Manso [81], K. Røed [22], E. Rogochaya [66], D. Rohr [43], D. Röhrich [18], R. Romita [124], F. Ronchetti [72,36], L. Ronflette [113], P. Rosnet [70], A. Rossi [30,36], F. Roukoutakis [88], A. Roy [49], C. Roy [55], P. Roy [100], A.J. Rubio Montero [10], R. Rui [26], R. Russo [27], E. Ryabinkin [99], Y. Ryabov [85], A. Rybicki [117], S. Sadovsky [111], K. Šafařík [36], B. Sahlmuller [53], P. Sahoo [49], R. Sahoo [49], S. Sahoo [61], P.K. Sahu [61], J. Saini [132], S. Sakai [72], M.A. Saleh [134], J. Salzwedel [20], S. Sambyal [90], V. Samsonov [85], L. Šándor [59], A. Sandoval [64], M. Sano [128], D. Sarkar [132], E. Scapparone [104], F. Scarlassara [30], C. Schiaua [78], R. Schicker [93], C. Schmidt [96], H.R. Schmidt [35], S. Schuchmann [53], J. Schukraft [36], M. Schulc [40], T. Schuster [136], Y. Schutz [113,36], K. Schwarz [96], K. Schweda [96], G. Scioli [28], E. Scomparin [110], R. Scott [125], M. Šefčík [41], J.E. Seger [86], Y. Sekiguchi [127], D. Sekihata [47], I. Selyuzhenkov [96], K. Senosi [65], S. Senyukov [3,36], E. Serradilla [10,64], A. Sevcenco [62], A. Shabanov [56], A. Shabetai [113], O. Shadura [3], R. Shahoyan [36], A. Shangaraev [111], A. Sharma [90], M. Sharma [90], M. Sharma [90], N. Sharma [125], K. Shigaki [47], K. Shtejer [9,27], Y. Sibiriak [99], S. Siddhanta [105], K.M. Sielewicz [36], T. Siemiarczuk [77], D. Silvermyr [84,34], C. Silvestre [71], G. Simatovic [129], G. Simonetti [36], R. Singaraju [132], R. Singh [79], S. Singha [132,79], V. Singhal [132], B.C. Sinha [132], T. Sinha [100], B. Sitar [39], M. Sitta [32], T.B. Skaali [22], M. Slupecki [123], N. Smirnov [136], R.J.M. Snellings [57], T.W. Snellman [123], C. Søgaard [34], J. Song [95], M. Song [137], Z. Song [7], F. Soramel [30], S. Sorensen [125], F. Sozzi [96], M. Spacek [40], E. Spiriti [72], I. Sputowska [117], M. Spyropoulou-Stassinaki [88], J. Stachel [93], I. Stan [62], G. Stefanek [77], E. Stenlund [34], G. Steyn [65], J.H. Stiller [93], D. Stocco [113], P. Strmen [39], A.A.P. Suaide [120], T. Sugitate [47], C. Suire [51], M. Suleymanov [16], M. Suljic [26,i], R. Sultanov [58], M. Šumbera [83], A. Szabo [39], A. Szanto de Toledo [120,i], I. Szarka [39], A. Szczepankiewicz [36], M. Szymanski [133], U. Tabassam [16], J. Takahashi [121], G.J. Tambave [18], N. Tanaka [128], M.A. Tangaro [33], M. Tarhini [51], M. Tariq [19], M.G. Tarzila [78], A. Tauro [36], G. Tejeda Muñoz [2], A. Telesca [36], K. Terasaki [127], C. Terrevoli [30], B. Teyssier [130], J. Thäder [74], D. Thomas [118], R. Tieulent [130], A.R. Timmins [122], A. Toia [53], S. Trogolo [27], G. Trombetta [33], V. Trubnikov [3], W.H. Trzaska [123], T. Tsuji [127], A. Tumkin [98], R. Turrisi [107], T.S. Tveter [22], K. Ullaland [18], A. Uras [130], G.L. Usai [25], A. Utrobicic [129], M. Vajzer [83], M. Vala [59], L. Valencia Palomo [70], S. Vallero [27], J. Van Der Maarel [57], J.W. Van Hoorne [36], M. van Leeuwen [57], T. Vanat [83], P. Vande Vyvre [36], D. Varga [135], A. Vargas [2], M. Vargyas [123], R. Varma [48], M. Vasileiou [88], A. Vasiliev [99], A. Vauthier [71], V. Vechernin [131], A.M. Veen [57], M. Veldhoen [57], A. Velure [18], M. Venaruzzo [73], E. Vercellin [27], S. Vergara Limón [2], R. Vernet [8], M. Verweij [134], L. Vickovic [116], G. Viesti [30,i], J. Viinikainen [123], Z. Vilakazi [126], O. Villalobos Baillie [101], A. Villatoro Tello [2], A. Vinogradov [99], L. Vinogradov [131], Y. Vinogradov [98,i], T. Virgili [31], V. Vislavicius [34], Y.P. Viyogi [132], A. Vodopyanov [66], M.A. Völkl [93], K. Voloshin [58], S.A. Voloshin [134], G. Volpe [135], B. von Haller [36], I. Vorobyev [37,92], D. Vranic [96,36], J. Vrláková [41], B. Vulpescu [70], A. Vyushin [98], B. Wagner [18], J. Wagner [96], H. Wang [57], M. Wang [7,113], D. Watanabe [128], Y. Watanabe [127], M. Weber [112,36], S.G. Weber [96], D.F. Weiser [93], J.P. Wessels [54], U. Westerhoff [54], A.M. Whitehead [89], J. Wiechula [35], J. Wikne [22], M. Wilde [54], G. Wilk [77], J. Wilkinson [93], M.C.S. Williams [104], B. Windelband [93], M. Winn [93], C.G. Yaldo [134], H. Yang [57], P. Yang [7], S. Yano [47], C. Yasar [69], Z. Yin [7], H. Yokoyama [128], I.-K. Yoo [95], J.H. Yoon [50], V. Yurchenko [3], I. Yushmanov [99], A. Zaborowska [133], V. Zaccolo [80], A. Zaman [16], C. Zampolli [104], H.J.C. Zanoli [120], S. Zaporozhets [66], N. Zardoshti [101], A. Zarochentsev [131], P. Závada [60], N. Zaviyalov [98], H. Zbroszczyk [133], I.S. Zgura [62], M. Zhalov [85], H. Zhang [18], X. Zhang [74], Y. Zhang [7], C. Zhang [57], Z. Zhang [7], C. Zhao [22], N. Zhigareva [58],

D. Zhou [7], Y. Zhou [80], Z. Zhou [18], H. Zhu [18], J. Zhu [113,7], A. Zichichi [28,12], A. Zimmermann [93],
M.B. Zimmermann [54,36], G. Zinovjev [3], M. Zyzak [43]

[1] *A.I. Alikhanyan National Science Laboratory (Yerevan Physics Institute) Foundation, Yerevan, Armenia*
[2] *Benemérita Universidad Autónoma de Puebla, Puebla, Mexico*
[3] *Bogolyubov Institute for Theoretical Physics, Kiev, Ukraine*
[4] *Bose Institute, Department of Physics and Centre for Astroparticle Physics and Space Science (CAPSS), Kolkata, India*
[5] *Budker Institute for Nuclear Physics, Novosibirsk, Russia*
[6] *California Polytechnic State University, San Luis Obispo, CA, United States*
[7] *Central China Normal University, Wuhan, China*
[8] *Centre de Calcul de l'IN2P3, Villeurbanne, France*
[9] *Centro de Aplicaciones Tecnológicas y Desarrollo Nuclear (CEADEN), Havana, Cuba*
[10] *Centro de Investigaciones Energéticas Medioambientales y Tecnológicas (CIEMAT), Madrid, Spain*
[11] *Centro de Investigación y de Estudios Avanzados (CINVESTAV), Mexico City and Mérida, Mexico*
[12] *Centro Fermi – Museo Storico della Fisica e Centro Studi e Ricerche "Enrico Fermi", Rome, Italy*
[13] *Chicago State University, Chicago, IL, USA*
[14] *China Institute of Atomic Energy, Beijing, China*
[15] *Commissariat à l'Energie Atomique, IRFU, Saclay, France*
[16] *COMSATS Institute of Information Technology (CIIT), Islamabad, Pakistan*
[17] *Departamento de Física de Partículas and IGFAE, Universidad de Santiago de Compostela, Santiago de Compostela, Spain*
[18] *Department of Physics and Technology, University of Bergen, Bergen, Norway*
[19] *Department of Physics, Aligarh Muslim University, Aligarh, India*
[20] *Department of Physics, Ohio State University, Columbus, OH, United States*
[21] *Department of Physics, Sejong University, Seoul, South Korea*
[22] *Department of Physics, University of Oslo, Oslo, Norway*
[23] *Dipartimento di Elettrotecnica ed Elettronica del Politecnico, Bari, Italy*
[24] *Dipartimento di Fisica dell'Università 'La Sapienza' and Sezione INFN, Rome, Italy*
[25] *Dipartimento di Fisica dell'Università and Sezione INFN, Cagliari, Italy*
[26] *Dipartimento di Fisica dell'Università and Sezione INFN, Trieste, Italy*
[27] *Dipartimento di Fisica dell'Università and Sezione INFN, Turin, Italy*
[28] *Dipartimento di Fisica e Astronomia dell'Università and Sezione INFN, Bologna, Italy*
[29] *Dipartimento di Fisica e Astronomia dell'Università and Sezione INFN, Catania, Italy*
[30] *Dipartimento di Fisica e Astronomia dell'Università and Sezione INFN, Padova, Italy*
[31] *Dipartimento di Fisica 'E.R. Caianiello' dell'Università and Gruppo Collegato INFN, Salerno, Italy*
[32] *Dipartimento di Scienze e Innovazione Tecnologica dell'Università del Piemonte Orientale and Gruppo Collegato INFN, Alessandria, Italy*
[33] *Dipartimento Interateneo di Fisica 'M. Merlin' and Sezione INFN, Bari, Italy*
[34] *Division of Experimental High Energy Physics, University of Lund, Lund, Sweden*
[35] *Eberhard Karls Universität Tübingen, Tübingen, Germany*
[36] *European Organization for Nuclear Research (CERN), Geneva, Switzerland*
[37] *Excellence Cluster Universe, Technische Universität München, Munich, Germany*
[38] *Faculty of Engineering, Bergen University College, Bergen, Norway*
[39] *Faculty of Mathematics, Physics and Informatics, Comenius University, Bratislava, Slovakia*
[40] *Faculty of Nuclear Sciences and Physical Engineering, Czech Technical University in Prague, Prague, Czech Republic*
[41] *Faculty of Science, P.J. Šafárik University, Košice, Slovakia*
[42] *Faculty of Technology, Buskerud and Vestfold University College, Vestfold, Norway*
[43] *Frankfurt Institute for Advanced Studies, Johann Wolfgang Goethe-Universität Frankfurt, Frankfurt, Germany*
[44] *Gangneung-Wonju National University, Gangneung, South Korea*
[45] *Gauhati University, Department of Physics, Guwahati, India*
[46] *Helsinki Institute of Physics (HIP), Helsinki, Finland*
[47] *Hiroshima University, Hiroshima, Japan*
[48] *Indian Institute of Technology Bombay (IIT), Mumbai, India*
[49] *Indian Institute of Technology Indore, Indore (IITI), India*
[50] *Inha University, Incheon, South Korea*
[51] *Institut de Physique Nucléaire d'Orsay (IPNO), Université Paris-Sud, CNRS-IN2P3, Orsay, France*
[52] *Institut für Informatik, Johann Wolfgang Goethe-Universität Frankfurt, Frankfurt, Germany*
[53] *Institut für Kernphysik, Johann Wolfgang Goethe-Universität Frankfurt, Frankfurt, Germany*
[54] *Institut für Kernphysik, Westfälische Wilhelms-Universität Münster, Münster, Germany*
[55] *Institut Pluridisciplinaire Hubert Curien (IPHC), Université de Strasbourg, CNRS-IN2P3, Strasbourg, France*
[56] *Institute for Nuclear Research, Academy of Sciences, Moscow, Russia*
[57] *Institute for Subatomic Physics of Utrecht University, Utrecht, Netherlands*
[58] *Institute for Theoretical and Experimental Physics, Moscow, Russia*
[59] *Institute of Experimental Physics, Slovak Academy of Sciences, Košice, Slovakia*
[60] *Institute of Physics, Academy of Sciences of the Czech Republic, Prague, Czech Republic*
[61] *Institute of Physics, Bhubaneswar, India*
[62] *Institute of Space Science (ISS), Bucharest, Romania*
[63] *Instituto de Ciencias Nucleares, Universidad Nacional Autónoma de México, Mexico City, Mexico*
[64] *Instituto de Física, Universidad Nacional Autónoma de México, Mexico City, Mexico*
[65] *iThemba LABS, National Research Foundation, Somerset West, South Africa*
[66] *Joint Institute for Nuclear Research (JINR), Dubna, Russia*
[67] *Konkuk University, Seoul, South Korea*
[68] *Korea Institute of Science and Technology Information, Daejeon, South Korea*
[69] *KTO Karatay University, Konya, Turkey*
[70] *Laboratoire de Physique Corpusculaire (LPC), Clermont Université, Université Blaise Pascal, CNRS-IN2P3, Clermont-Ferrand, France*
[71] *Laboratoire de Physique Subatomique et de Cosmologie, Université Grenoble-Alpes, CNRS-IN2P3, Grenoble, France*
[72] *Laboratori Nazionali di Frascati, INFN, Frascati, Italy*
[73] *Laboratori Nazionali di Legnaro, INFN, Legnaro, Italy*
[74] *Lawrence Berkeley National Laboratory, Berkeley, CA, United States*
[75] *Moscow Engineering Physics Institute, Moscow, Russia*

[76] *Nagasaki Institute of Applied Science, Nagasaki, Japan*
[77] *National Centre for Nuclear Studies, Warsaw, Poland*
[78] *National Institute for Physics and Nuclear Engineering, Bucharest, Romania*
[79] *National Institute of Science Education and Research, Bhubaneswar, India*
[80] *Niels Bohr Institute, University of Copenhagen, Copenhagen, Denmark*
[81] *Nikhef, Nationaal instituut voor subatomaire fysica, Amsterdam, Netherlands*
[82] *Nuclear Physics Group, STFC Daresbury Laboratory, Daresbury, United Kingdom*
[83] *Nuclear Physics Institute, Academy of Sciences of the Czech Republic, Řež u Prahy, Czech Republic*
[84] *Oak Ridge National Laboratory, Oak Ridge, TN, United States*
[85] *Petersburg Nuclear Physics Institute, Gatchina, Russia*
[86] *Physics Department, Creighton University, Omaha, NE, United States*
[87] *Physics Department, Panjab University, Chandigarh, India*
[88] *Physics Department, University of Athens, Athens, Greece*
[89] *Physics Department, University of Cape Town, Cape Town, South Africa*
[90] *Physics Department, University of Jammu, Jammu, India*
[91] *Physics Department, University of Rajasthan, Jaipur, India*
[92] *Physik Department, Technische Universität München, Munich, Germany*
[93] *Physikalisches Institut, Ruprecht-Karls-Universität Heidelberg, Heidelberg, Germany*
[94] *Purdue University, West Lafayette, IN, United States*
[95] *Pusan National University, Pusan, South Korea*
[96] *Research Division and ExtreMe Matter Institute EMMI, GSI Helmholtzzentrum für Schwerionenforschung, Darmstadt, Germany*
[97] *Rudjer Bošković Institute, Zagreb, Croatia*
[98] *Russian Federal Nuclear Center (VNIIEF), Sarov, Russia*
[99] *Russian Research Centre Kurchatov Institute, Moscow, Russia*
[100] *Saha Institute of Nuclear Physics, Kolkata, India*
[101] *School of Physics and Astronomy, University of Birmingham, Birmingham, United Kingdom*
[102] *Sección Física, Departamento de Ciencias, Pontificia Universidad Católica del Perú, Lima, Peru*
[103] *Sezione INFN, Bari, Italy*
[104] *Sezione INFN, Bologna, Italy*
[105] *Sezione INFN, Cagliari, Italy*
[106] *Sezione INFN, Catania, Italy*
[107] *Sezione INFN, Padova, Italy*
[108] *Sezione INFN, Rome, Italy*
[109] *Sezione INFN, Trieste, Italy*
[110] *Sezione INFN, Turin, Italy*
[111] *SSC IHEP of NRC Kurchatov Institute, Protvino, Russia*
[112] *Stefan Meyer Institut für Subatomare Physik (SMI), Vienna, Austria*
[113] *SUBATECH, Ecole des Mines de Nantes, Université de Nantes, CNRS-IN2P3, Nantes, France*
[114] *Suranaree University of Technology, Nakhon Ratchasima, Thailand*
[115] *Technical University of Košice, Košice, Slovakia*
[116] *Technical University of Split FESB, Split, Croatia*
[117] *The Henryk Niewodniczanski Institute of Nuclear Physics, Polish Academy of Sciences, Cracow, Poland*
[118] *The University of Texas at Austin, Physics Department, Austin, TX, USA*
[119] *Universidad Autónoma de Sinaloa, Culiacán, Mexico*
[120] *Universidade de São Paulo (USP), São Paulo, Brazil*
[121] *Universidade Estadual de Campinas (UNICAMP), Campinas, Brazil*
[122] *University of Houston, Houston, TX, United States*
[123] *University of Jyväskylä, Jyväskylä, Finland*
[124] *University of Liverpool, Liverpool, United Kingdom*
[125] *University of Tennessee, Knoxville, TN, United States*
[126] *University of the Witwatersrand, Johannesburg, South Africa*
[127] *University of Tokyo, Tokyo, Japan*
[128] *University of Tsukuba, Tsukuba, Japan*
[129] *University of Zagreb, Zagreb, Croatia*
[130] *Université de Lyon, Université Lyon 1, CNRS/IN2P3, IPN-Lyon, Villeurbanne, France*
[131] *V. Fock Institute for Physics, St. Petersburg State University, St. Petersburg, Russia*
[132] *Variable Energy Cyclotron Centre, Kolkata, India*
[133] *Warsaw University of Technology, Warsaw, Poland*
[134] *Wayne State University, Detroit, MI, United States*
[135] *Wigner Research Centre for Physics, Hungarian Academy of Sciences, Budapest, Hungary*
[136] *Yale University, New Haven, CT, United States*
[137] *Yonsei University, Seoul, South Korea*
[138] *Zentrum für Technologietransfer und Telekommunikation (ZTT), Fachhochschule Worms, Worms, Germany*

[i] Deceased.
[ii] Also at: Georgia State University, Atlanta, Georgia, United States.
[iii] Also at: M.V. Lomonosov Moscow State University, D.V. Skobeltsyn Institute of Nuclear, Physics, Moscow, Russia.